Molecular Therapy
Methods & Clinical Development
Original Article

Suprachoroidal and Subretinal Injections of AAV Using Transscleral Microneedles for Retinal Gene Delivery in Nonhuman Primates

Glenn Yiu,[1] Sook Hyun Chung,[1] Iris N. Mollhoff,[1] Uyen Tu Nguyen,[1] Sara M. Thomasy,[1,2] Jesse Yoo,[3] Donna Taraborelli,[3] and Glenn Noronha[3]

[1]Department of Ophthalmology & Vision Science, University of California, Davis, 4860 Y Street, Suite 2400, Sacramento, CA 95817, USA; [2]Department of Surgical and Radiological Sciences, School of Veterinary Medicine, University of California, Davis, 1 Garrod Drive, Davis, CA 95616, USA; [3]Clearside Biomedical, 900 North Point Parkway, Suite 200, Alpharetta, GA 30005, USA

Retinal gene therapy using adeno-associated viruses (AAVs) is constrained by the mode of viral vector delivery. Intravitreal AAV injections are impeded by the internal limiting membrane barrier, while subretinal injections require invasive surgery and produce a limited region of therapeutic effect. In this study, we introduce a novel mode of ocular gene delivery in rhesus macaques using transscleral microneedles to inject AAV8 into the subretinal or suprachoroidal space, a potential space between the choroid and scleral wall of the eye. Using *in vivo* imaging, we found that suprachoroidal AAV8 produces diffuse, peripheral expression in retinal pigment epithelial (RPE) cells, but it elicited local infiltration of inflammatory cells. Transscleral subretinal injection of AAV8 using microneedles leads to focal gene expression with transduction of RPE and photoreceptors, and minimal intraocular inflammation. In comparison, intravitreal AAV8 shows minimal transduction of retinal cells, but elicits greater systemic humoral immune responses. Our study introduces a novel mode of transscleral viral delivery that can be performed without vitreoretinal surgery, with focal or diffuse transgene expression patterns suitable for different applications. The decoupling of local and systemic immune responses reveals important insights into the immunological consequences of AAV delivery to different ocular compartments surrounding the blood-retinal barrier.

INTRODUCTION

The use of adeno-associated viral (AAV) vectors has been instrumental in the development of ocular gene therapies for treating inherited retinal diseases and complex degenerative retinal conditions. AAVs are nonpathogenic, replication-deficient, and exhibit low immunogenicity. They also have the ability to infect different retinal cell types, making them efficient vectors for gene transfer in the eye.[1] Recombinant AAV can encode a promoter and therapeutic transgene cassette up to 4.7 kb flanked by AAV inverted terminal repeats for replication and packaging. Transduction efficiency and tissue tropism are determined by the capsid,[2] with hundreds of AAV variants described to date.[3,4] The first US Food and Drug Administration (FDA)-approved gene therapy for the eye employs AAV2 to express the RPE65 gene encoding a retinal isomerase to treat patients with biallelic RPE65 mutation-associated retinal dystrophy, a rare retinal condition characterized by severe visual impairment that begins during infancy.[5–10] Similar gene therapy strategies have also been developed for retinitis pigmentosa,[11–13] achromatopsia,[14,15] X-linked retinoschisis,[16,17] and neovascular forms of age-related macular degeneration (AMD),[18–20] with many ongoing clinical trials underway.

Many current retinal gene therapy protocols employ subretinal injection of the AAV vector, which involves vitrectomy surgery and insertion of a cannula through the retina to create a retinotomy to deliver the viral particles to photoreceptors and/or underlying retinal pigment epithelium (RPE). Compared to systemic delivery, AAV in the subretinal space elicits a reduced immune response compared to systemic delivery, similar to the anterior chamber-associated immune deviation (ACAID) that enables corneal transplantation without immunosuppression.[21,22] However, the technique is more difficult and subject to potential complications of vitrectomy surgery such as retinal tear, retinal detachment, the need for more eye surgery, cataract, intraocular pressure abnormalities, and intraocular infection.[23,24] The focal injection of AAV particles also limits the therapeutic effect to a small region near the injection site. Furthermore, because these subretinal injections must be performed in an operating room with a surgical microscope, access is costly for patients and repeated treatments are difficult.

Intravitreal injections can overcome some of the limitations of subretinal delivery, and they are frequently performed in office settings by ophthalmologists to deliver anti-angiogenesis agents for treating

Received 13 December 2019; accepted 6 January 2020;
https://doi.org/10.1016/j.omtm.2020.01.002.

Correspondence: Glenn Yiu, MD, PhD, Department of Ophthalmology & Vision Science, University of California, Davis, 4860 Y Street, Suite 2400, Sacramento, CA 95817, USA.
E-mail: gyiu@ucdavis.edu

neovascular retinal conditions.[25] However, the internal limiting membrane (ILM) limits the penetration of the current generation of AAV vectors, and transduction is often limited to inner retinal layers.[26] Although surgical removal of the ILM can enhance AAV transduction from the vitreous,[27,28] vitrectomy is necessary for this procedure. Novel AAV variants identified by *in vivo*-directed evolution[29] or mutation of capsid tyrosines[30] may also improve transduction of the outer retina, but efficacy in murine eyes does not reliably predict effectiveness in primates. Also, intravitreal AAV causes more intraocular inflammation and elicits a more potent humoral immune response than does subretinal administration.[31–34]

The suprachoroidal space is the potential space located between the choroidal vasculature and the scleral wall of the eye. In humans, this layer is rarely detectable except in pathologic conditions when accumulation of suprachoroidal fluid becomes visible on ultrasonography,[35] although advances in spectral domain-optical coherence tomography (SD-OCT) allow the space to be visualized in some healthy eyes also.[36,37] Suprachoroidal delivery of pharmacologic agents has been explored for targeted delivery to chorioretinal tissues with improved pharmacokinetics and duration.[38] Suprachoroidal delivery can be achieved by surgical cannulation[39] or transscleral microneedles[40,41] that are only long enough to penetrate the sclera without perforating the retina (Figure 1A). In clinical studies, suprachoroidal injection of triamcinolone acetonide suspension using microneedles showed efficacy in treating noninfectious uveitis and retinal vein occlusions.[42,43]

In this study, we report the novel use of transscleral microneedles to deliver AAV vectors to the subretinal or suprachoroidal space using a nonhuman primate model. While common laboratory rodents have a large lens relative to the size of the eye, a thin sclera, and ocular dimensions that are too small for reliably accessing the suprachoroidal space, rhesus macaques have ocular dimensions and vascular architecture that are nearly identical to humans.[44,45] Using AAV8, which has been shown to effectively transduce photoreceptors and RPE,[46] we found that suprachoroidal AAV8 delivery produced diffuse, peripheral transduction of mostly RPE, while subretinal injection using transscleral microneedles led to a robust, but localized area of gene transfer to multiple retinal cell types. Without systemic immunosuppression, suprachoroidal AAV8 also elicited local infiltration of inflammatory cells in the outer retina and choroid, but less vitreous inflammation or systemic humoral immune responses. Our results demonstrate distinct expression patterns of subretinal and suprachoroidal AAV delivery using transscleral microneedles that may be suitable for different potential applications of retinal gene therapy, and they highlight the immune consequences of AAV exposure to different ocular compartments bordering the blood-retinal barrier (BRB). These findings suggest that suprachoroidal AAV injections may be a promising, novel route for ocular gene delivery, if the potential immune complications of this technique can be adequately addressed.

RESULTS

Suprachoroidal AAV8 Transduction Is Diffuse, Peripheral, and Circumferential

We screened 24 rhesus macaques (4–10 years of age) for absence of pre-existing serum neutralizing antibodies (NAbs) to AAV8 using an *in vitro* transduction inhibition assay,[47] and identified 6 animals (mean age, 8.3 ± 2.4 years; 3 males/3 females) with no detectable NAbs (<1:2,560), consistent with the high prevalence of anti-AAV8 NAbs reported in rhesus macaques.[48] We injected both eyes of three of these animals with nonhuman primate-grade AAV8 expressing enhanced green fluorescent protein (GFP) under a ubiquitous cytomegalovirus (CMV) promoter at two different doses (7×10^{11} or 7×10^{12} vector genomes [vg]/eye) using a 700-μm-long 30-gauge microneedle (Figure 1B, Clearside Biomedical, Alpharetta, GA, USA) inserted through the conjunctiva and sclera into the suprachoroidal space in the superotemporal quadrant (single 100-μL injection) of left eyes, and both superotemporal and inferonasal quadrants (two 50-μL injections) of right eyes (Figure 1C). No surgical microscope or vitrectomy surgery was required. Animals were scheduled for *in vivo* fluorescence retinal imaging by scanning laser ophthalmoscopy (SLO) to measure GFP expression at 1 week, 1 month, and 3 months after AAV8 injection, followed by necropsy for histological analysis (Figure 1D). One of these animals (rhesus 00) was subsequently found to have existing NAbs and erroneously enrolled, and was excluded from further analyses. While the animal that received the lower dose (rhesus 01) showed no detectable expression at any time points, the animal injected with 7×10^{12} vg/eye (rhesus 02) exhibited scattered areas of punctate GFP fluorescence bilaterally in the peripheral fundus at 1 week (Figures 1E and 1H), which increased at 1 month (Figures 1F and 1I), but was not detectable at 3 months (Figures 1G and 1J). Although the facial contour of rhesus monkeys limits our steering of the SLO device to image some quadrants of the peripheral retina, GFP expression was near circumferential, with no predilection for the injection location or quadrant. These results suggest that suprachoroidal delivery of AAV8 results in diffuse and peripheral expression of the GFP transgene, although durability may be limited.

Comparison of Suprachoroidal, Subretinal, and Intravitreal AAV8 Transduction *In Vivo*

Based on results from these dose-ranging studies and given the peripheral pattern of expression, we adjusted our protocol to transsclerally inject more posteriorly at 10 mm posterior to the limbus (near the globe equator) using the microneedles, and inject one animal intravitreally for comparison using a standard 0.5-inch-long 30-gauge needle through the pars plana at 4 mm posterior to the limbus (Figure 1B). We also scheduled these animals to undergo necropsy earlier at months 1 and 2 after injection due to the GFP expression loss at month 3 (Figure 1D). Interestingly, we found that transscleral microneedle injections at this posterior location achieved subretinal AAV delivery in two eyes, as evidenced by a small spot of subretinal hemorrhage seen on funduscopic examination. Compared with suprachoroidal AAV8 (Figures 2A and 2D), subretinal delivery of AAV8 using this transscleral approach produced robust focal

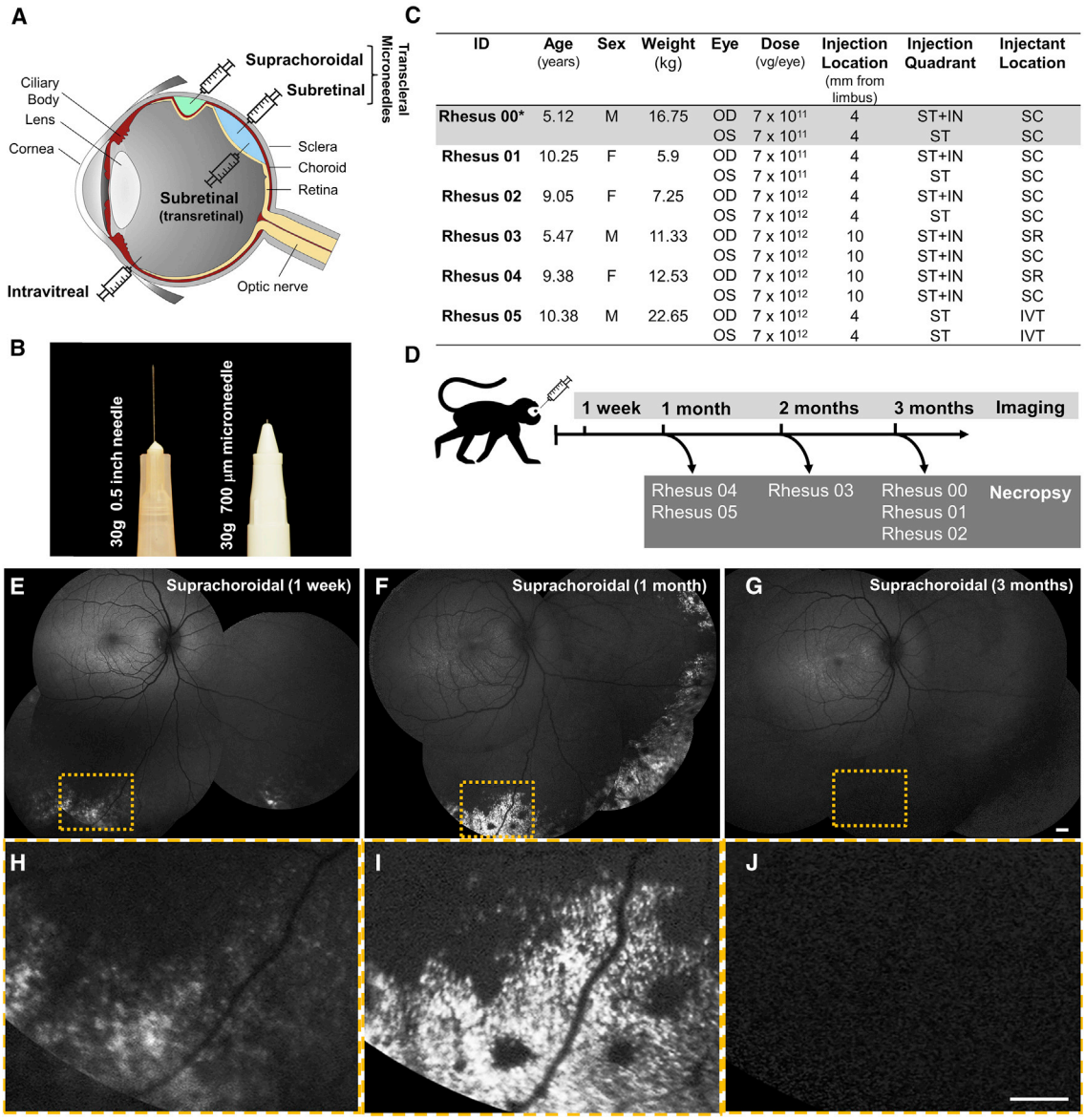

ID	Age (years)	Sex	Weight (kg)	Eye	Dose (vg/eye)	Injection Location (mm from limbus)	Injection Quadrant	Injectant Location
Rhesus 00*	5.12	M	16.75	OD	7×10^{11}	4	ST+IN	SC
				OS	7×10^{11}	4	ST	SC
Rhesus 01	10.25	F	5.9	OD	7×10^{11}	4	ST+IN	SC
				OS	7×10^{11}	4	ST	SC
Rhesus 02	9.05	F	7.25	OD	7×10^{12}	4	ST+IN	SC
				OS	7×10^{12}	4	ST	SC
Rhesus 03	5.47	M	11.33	OD	7×10^{12}	10	ST+IN	SR
				OS	7×10^{12}	10	ST+IN	SC
Rhesus 04	9.38	F	12.53	OD	7×10^{12}	10	ST+IN	SR
				OS	7×10^{12}	10	ST+IN	SC
Rhesus 05	10.38	M	22.65	OD	7×10^{12}	4	ST	IVT
				OS	7×10^{12}	4	ST	IVT

Figure 1. Experimental Design and *In Vivo* GFP Transgene Expression in Rhesus Macaque Eyes after Suprachoroidal Injection of AAV8

(A) Diagram of a primate eye showing different modes of AAV delivery, including intravitreal, subretinal (transretinal), and suprachoroidal or subretinal injections using transscleral microneedles. (B) Photograph comparing a standard 30-gauge needle with the transscleral microneedle used in this study. (C) Table outlining study animals and eyes, demographics, AAV8 dose, location and quadrant of injections, and the anatomic location of the injectant. *Rhesus 00 was found to have pre-existing AAV-neutralizing antibodies and was subsequently excluded. (D) Schematic of time points for ocular imaging and necropsy of study animals. (E–G) Scanning laser ophthalmoscopy (SLO) montages and (H–J) magnified views of the yellow-dashed boxes in (E–G) showing GFP expression at 1 week (E and H), 1 month (F and I), and 3 months (G and J) after AAV injections. Scale bars, 1 mm. F, female; M, male; OD, right eye; OS, left eye; IN, inferonasal; IVT, intravitreal; SC, suprachoroidal; SR, subretinal; ST, superotemporal; vg, viral genomes.

transduction near the injection site, with GFP expression visible in some retinal nerve fiber projections to the optic disc suggesting transduction of retinal ganglion neurons (Figures 2B and 2E). In contrast, intravitreal injection of the same dose of AAV8 showed only scant peripapillary expression mostly nasal to the optic disc (Figures 2C and 2F). Thus, without requiring vitrectomy surgery, transscleral microneedle injections allow both subretinal and suprachoroidal AAV delivery with distinct patterns of transduction, and they are more efficient than intravitreal injections of AAV8.

When comparing cross-sectional retinal morphology *in vivo* using SD-OCT, which correlates well with anatomic layers on

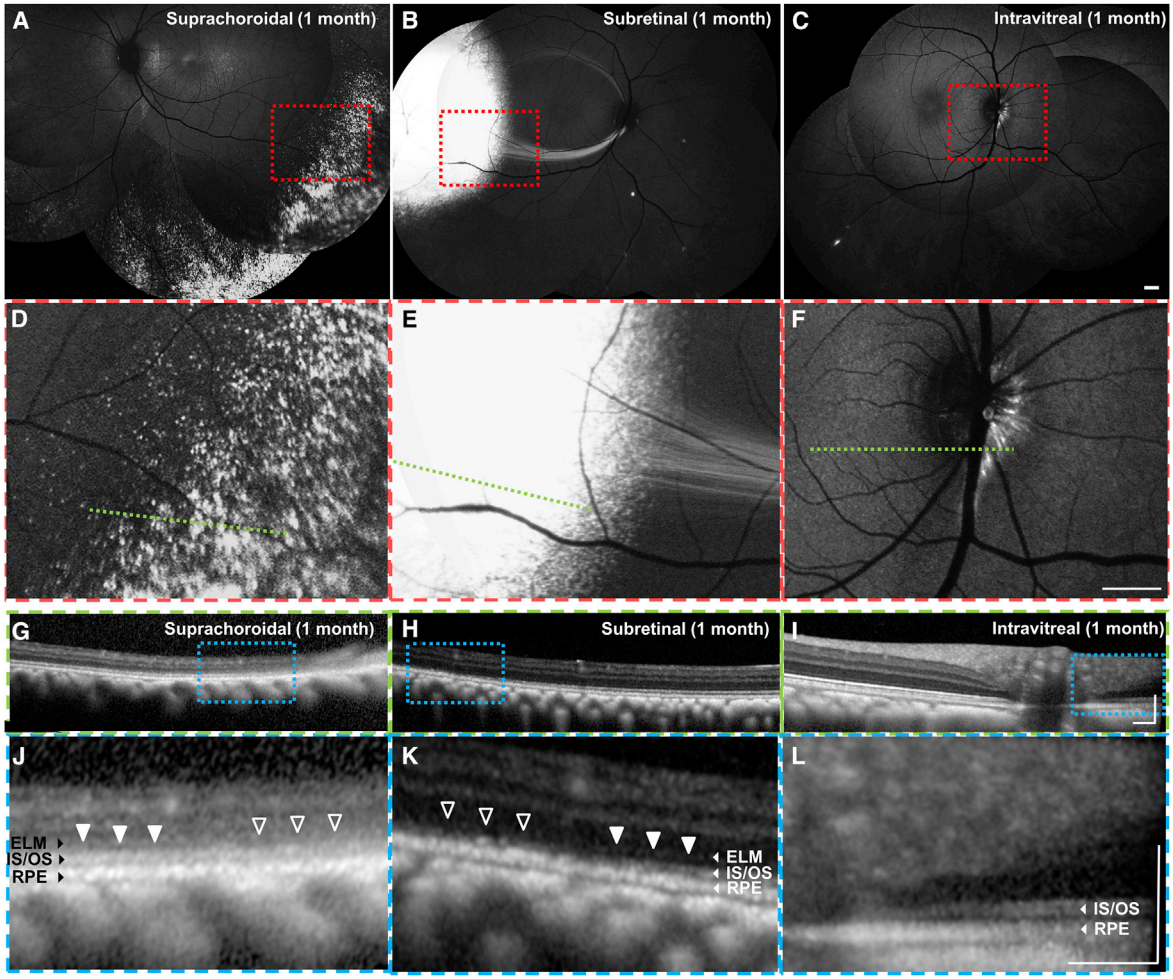

Figure 2. *In Vivo* GFP Transgene Expression after Suprachoroidal, Subretinal, and Intravitreal Injections of AAV8 in Rhesus Macaques

(A–C) Scanning laser ophthalmoscopy (SLO) montages and (D–F) magnified views of the red-dashed boxes in (A)–(C) showing different patterns of GFP expression after suprachoroidal (A and D), subretinal (B and E), and intravitreal (C and F) AAV injections. (G–I) Spectral domain-optical coherence tomography (SD-OCT) scans across the green dashed lines in (D)–(F), with (J–L) magnified views of the blue-dashed boxes in (G)–(I), showing impact on external limiting membrane (ELM), photoreceptor inner segment/outer segment junction (IS/OS), and retinal pigment epithelium (RPE) after suprachoroidal (G and J), subretinal (H and K), and intravitreal (I and L) AAV injections. ELM and IS/OS disruptions were seen in areas of greatest GFP transduction (open arrowheads) compared with adjacent areas with less transduction (closed arrowheads). Scale bars, 1 mm (A–F), 0.2 mm (G–L). ELM, external limiting membrane; IS/OS, inner segment/outer segment junction; RPE, retinal pigment epithelium.

histology,[45,49] we found that outer retinal layers, including photoreceptor inner segment/outer segment (IS/OS) junctions and external limiting membrane (ELM), appear disrupted in areas of highest GFP expression after suprachoroidal (Figures 2G and 2J) and subretinal (Figures 2H and 2K) injections, as compared to intravitreal AAV8 (Figures 2I and 2K). We note, however, that comparing retinal anatomy between these different modes of AAV injection may be difficult due to intrinsic differences in retinal morphology at the different locations of GFP expression (e.g., retinal layers are thinner and outer retinal bands are more difficult to discern on SD-OCT in peripheral retina as compared to posterior regions).

Retinal Cell Tropism and Anatomy after Suprachoroidal or Subretinal AAV8 Delivery

Histological analysis at 1 month confirmed the widespread GFP expression resulting from suprachoroidal AAV8 delivery (Figure 3A), compared to the more focal expression after subretinal AAV (Figure 3B) and scant expression after intravitreal AAV (Figure 3C) injections. The expression after suprachoroidal AAV8 was mostly in individual RPE cells (Figures 3D and 3G), corresponding to the punctate GFP fluorescence pattern *in vivo*. However, the RPE cells appear rounded and dysmorphic, with widespread disruption of photoreceptor inner and outer segments (Figures 3G and 3J). In contrast, subretinal AAV8 injection using transscleral microneedles

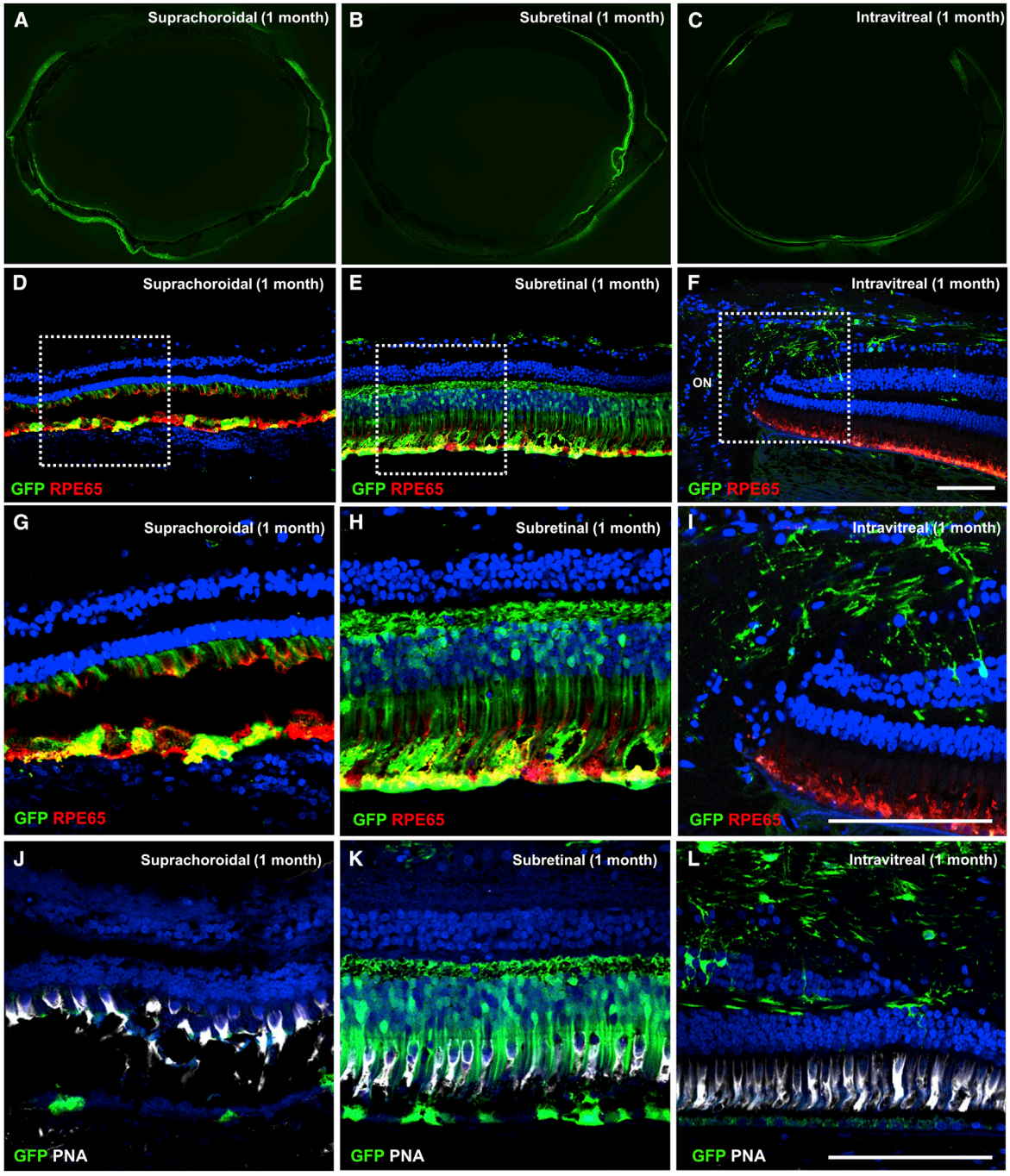

Figure 3. Retinal Cellular Tropism after Suprachoroidal, Subretinal, and Intravitreal Injection of AAV8 in Rhesus Macaques

(A–C) Epifluorescence image montages of entire globes showing different patterns of GFP transgene expression, and (D–F) confocal fluorescence images with (G–I) magnified views of the white-dashed boxes in (D)–(F) showing GFP transgene expression (green) co-immunostained with anti-RPE65 (red) to label retinal pigment epithelium (RPE), or (J–L) with peanut agglutinin (PNA, white) to label cone photoreceptor inner and outer segments, along with DAPI (blue) to label cell nuclei in eyes after suprachoroidal (A, D, G, and J), subretinal (B, E, H, and K), and intravitreal (C, F, I, and L) injections of AAV8-CMV-GFP. Scale bars, 100 μm.

efficiently transduced RPE, photoreceptors, and some retinal ganglion neurons, with better preservation of retinal anatomy (Figures 3E and 3H). Most of the transduced photoreceptors appear to be rods, based on cell morphology, preponderance of rods in the transduced area, and absence of co-staining with peanut agglutinin (PNA) (Figures 3K), which is consistent with past studies showing mostly

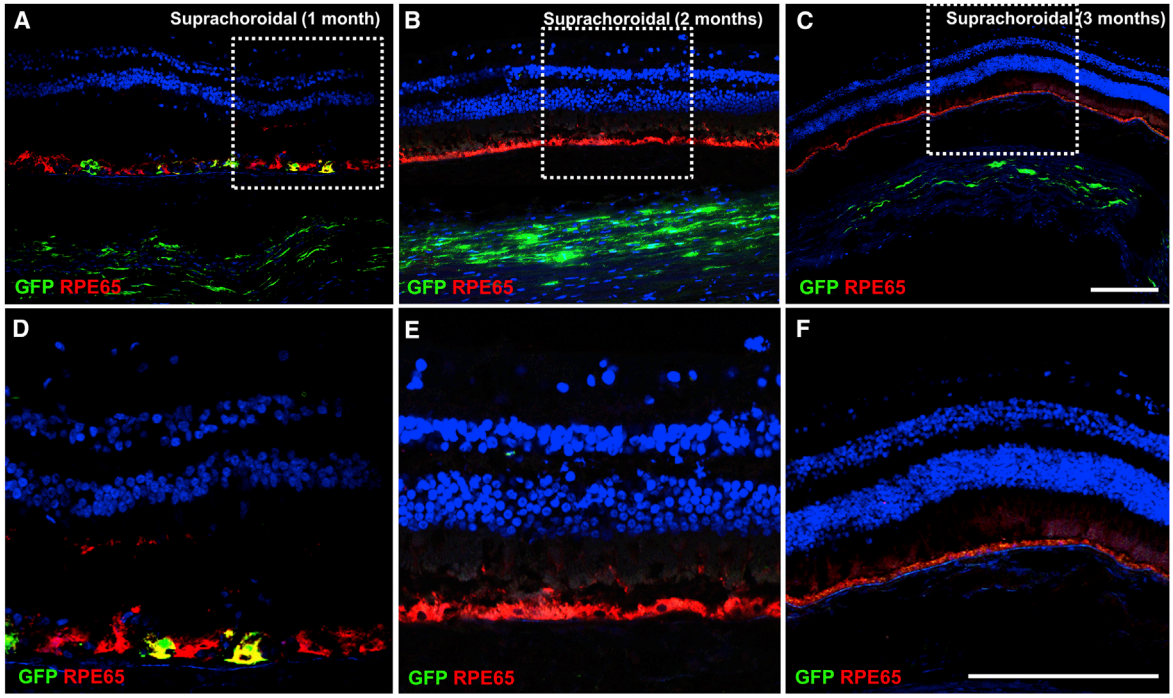

Figure 4. Transient GFP Expression in Retina and Choroid after Suprachoroidal AAV8 Delivery in Rhesus Macaques

(A–C) Confocal fluorescence images with (D–F) magnified views of the white-dashed boxes in (A)–(C) showing GFP transgene expression in the retinal pigment epithelium (RPE) and sclera (green) co-immunostained with anti-RPE65 (red) to label RPE and with DAPI (blue) to label cell nuclei in eyes at 1 month (A and D), 2 months (B and E), and 3 months (C and F) after suprachoroidal (SC) injection of AAV8-GFP. Scale bars, 100 μm.

rod transduction with standard transretinal subretinal AAV8 injections.[46] Intravitreal AAV8 showed only GFP expression in cells in the peripapillary region (Figures 3F, 3I, and 3L), with some colocalization with some glial fibrillary acidic protein (GFAP)$^+$ cells, which may include astrocytes or Müller glia based on their morphology and distribution. Photoreceptor and RPE morphologies were also more disorganized in regions closer to the injection site for both transscleral suprachoroidal and subretinal injections (Figure S1).

Consistent with the *in vivo* imaging data, GFP expression after suprachoroidal AAV8 injection was no longer present by months 2 and 3 (Figures 4A–4F), although GFP expression could still be detected in the sclera near the injection site (Figures 4A–4C), suggesting that the CMV promoter and expression cassette were still functional at these time points, and that the GFP$^+$ RPE cells were no longer present. While it is unclear if the GFP$^+$ cells in the sclera represent AAV-transduced cells or phagocytes containing cellular debris with the fluorescent protein, the absence of co-immunostaining with ionized calcium-binding adaptor-1 (Iba1), CD45, or GFAP in these regions supports the former alternative.

Ocular Inflammatory Responses after Different Modes of AAV8 Delivery

Both subretinal and suprachoroidal AAV8 injections using transscleral microneedles were well tolerated. There was no significant anterior chamber (AC) inflammation seen on slit lamp examination (Figure S2). Rhesus 02 exhibited behavioral signs of ocular irritation at week 2, was found to show mild AC cell (2+ based on the Standardization of Uveitis Nomenclature [SUN] criteria[50]), and was treated with oral prednisone (1 mg/kg) for 2 weeks with resolution of the inflammation by the month 1 examination. Subsequent animals were given a single 40-mg periorbital subtenon injection of triamcinolone and did not exhibit significant AC inflammation after injections (Table S1). None of the injected eyes exhibited significant intraocular pressure (IOP) elevation during the entirety of the study (Table S1), and funduscopic examination and photographs showed no visible vitreous haze in any eye throughout the study (Figure S3).

On histological analysis, suprachoroidal AAV8 delivery caused significant inflammatory infiltration with Iba1$^+$ cells in the outer retina and choroid (Figure 5A), likely representing a mix of retinal microglia and choroidal macrophages due to the disrupted RPE that normally constitutes the outer BRB. In contrast, transscleral subretinal AAV8 and intravitreal AAV8 showed minimal microglial activation compared to an uninjected control eye (Figures 5B–5D). Suprachoroidal AAV8 also triggered more profound CD45$^+$ leukocyte and CD3$^+$ T cell infiltration than did subretinal AAV8 (Figures 5E, 5F, 5I, and 5J), while almost none was seen after intravitreal AAV8 or in uninjected eyes (Figures 5G, 5H, 5K, and 5L), although the different inflammatory reactions may be related to the different location and patterns of

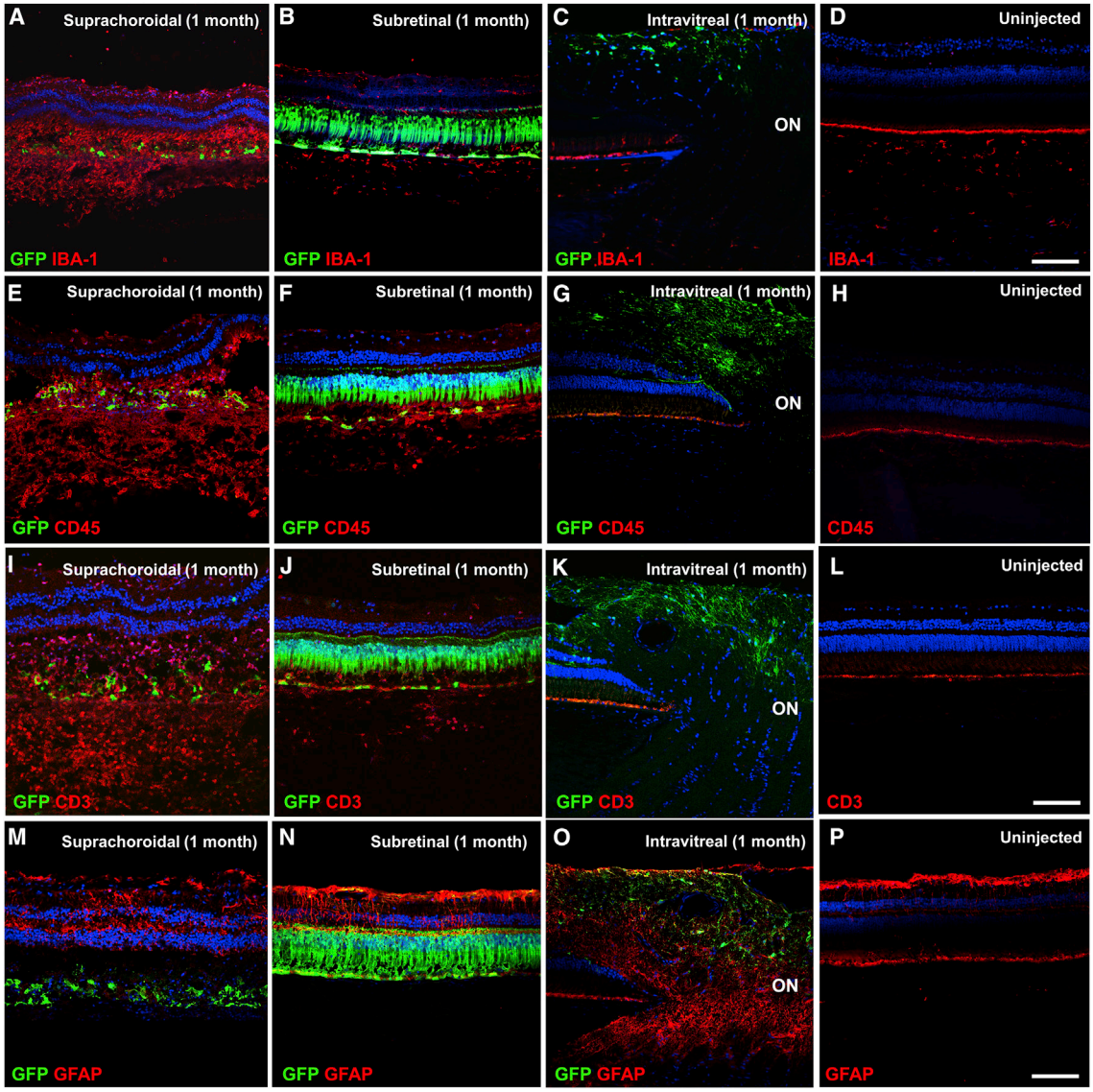

Figure 5. Local Inflammatory Response after Suprachoroidal, Subretinal, and Intravitreal Injection of AAV8 in Rhesus Macaques

(A–P) Confocal fluorescence images of GFP transgene expression (green) co-immunostained with anti-IBA-1 (red) to label retinal microglia and choroidal macrophages (A–D), anti-CD45 (red) to label infiltrating leukocytes (E–H), anti-CD3 (red) to label T cells (I–L), and anti-GFAP (red) to assess glial proliferation (M–P), in eyes that received suprachoroidal (A, E, I, and M), subretinal (B, F, J, and N), and intravitreal (C, G, K, and O) injections of AAV8-CMV-GFP, or uninjected control eyes (D, H, L, and P). Scale bars, 100 μm.

transgene expression. GFAP staining showed some reactive gliosis with disruption of Müller glia after suprachoroidal and subretinal AAV8 injections (Figures 5M–5P). Thus, suprachoroidal delivery of AAV vectors appears to trigger chorioretinitis with localized infiltration of inflammatory cells in the retina and choroid.

Humoral Immune Responses after Different Modes of AAV8 Delivery

Because the suprachoroidal space is outside the outer BRB, we evaluated whether AAV8 delivery to this compartment would elicit a greater systemic immune response than intravitreal AAV8 injections. Interestingly, animals that received suprachoroidal AAV8 using transscleral microneedles showed a less prominent NAb response that began at 1 week and remained stable up to 3 months (Figures 6A and 6C). In contrast, the animal that received intravitreal AAV8 demonstrated a more significant elevation in NAb titers at 1 month (Figures 6B and 6C), consistent with the response to intravitreal AAV8 in previous primate studies.[33,34] As predicted, the animal that received the lower dose of AAV8 in both eyes (7×10^{11} vg/eye) exhibited a milder NAb response. NAbs were

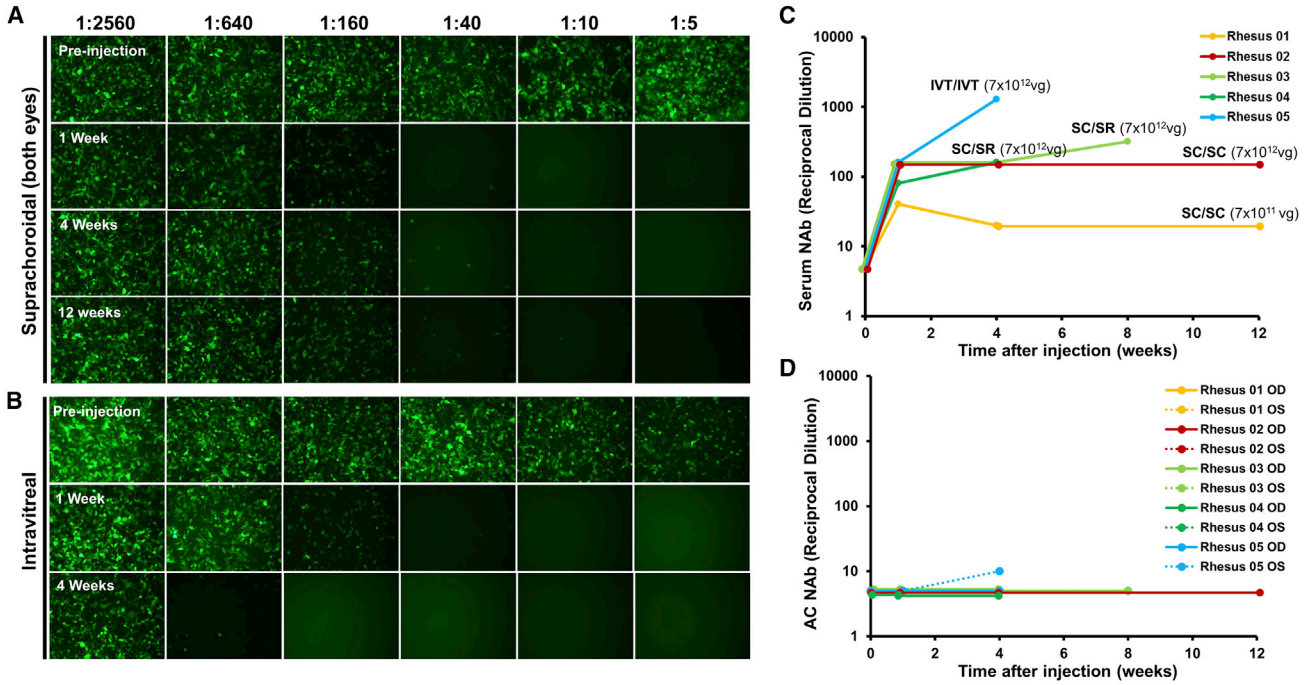

Figure 6. Host Humoral Immune Responses after Suprachoroidal or Intravitreal AAV8 Injections in Rhesus Macaques

(A and B) Epifluorescence images of HEK293T cells incubated with macaque serum and AAV8-CMV-GFP to detect serum neutralizing antibodies (NAbs) before and after suprachoroidal (SC/SC) (A) or intravitreal (IVT/IVT) (B) AAV8 injections. (C and D) Line graphs comparing serum (C) and aqueous (D) NAb titers in each study animal after AAV8 injections. The AAV8 injection mode and dose are labeled in (C). IVT, intravitreal; SC, suprachoroidal; SR, subretinal.

not detectable in aqueous samples of any study animals (Figure 6D). This corresponds to Goldmann-Witmer (G-W) ratio below 4 in all eyes, which indicates minimal intraocular inflammation as detected from the aqueous after all modes of AAV injection in our study. Since past studies did not show a significant NAb response after subretinal AAV8 alone,[33,34] and because the animals that received suprachoroidal and subretinal injection in fellow eyes (rhesus 03 and rhesus 04) showed a similar NAb response as animals that received bilateral suprachoroidal injections, the humoral immune response in these animals likely arose primarily from the suprachoroidal AAV8.

DISCUSSION

Current gene therapy approaches often employ subretinal injection of AAV vectors to allow direct access to photoreceptors and RPE for effective gene transfer, and to exploit the relative immune privilege of the subretinal space to minimize ocular inflammation. However, subretinal injections are usually performed through the retina (transretinally), requiring vitrectomy surgery and an operating microscope for visualization. The procedure is invasive, costly, and difficult to repeat frequently, and the area of gene transfer using current techniques may be localized to a small region near the injection site. Intravitreal injections are easier to perform, but conventional AAV serotypes have limited access to the outer retina due to the ILM barrier,[26] and they may trigger more vitreous inflammation and host humoral immune responses.[31,32]

Our study demonstrates a novel mode of transscleral viral vector delivery that can be performed in an office setting without surgery. By injecting the AAV through the scleral wall to the subretinal or suprachoroidal space, the technique provides more robust transgene expression than do intravitreal injections and different patterns of expression that may be suitable for different gene therapy applications. Similar to transretinal injections, transscleral microneedle injections into the subretinal space produce focal gene transfer to various cell types, including photoreceptors and RPE, with some retinal ganglion cells near the injection site that may have resulted from mechanical penetration of the microneedle into the inner retina. By avoiding vitrectomy surgery or the need to create a retinotomy, however, transscleral injections are easier to perform and less invasive, with reduced risks of iatrogenic retinal tears, retinal detachment, or other potential complications of vitreoretinal surgery. Unlike subretinal injections, suprachoroidal AAV delivery provides diffuse, widespread expression in peripheral RPE. The circumferential GFP expression pattern reflects the anatomy of the choroidal-scleral junction, which is more readily separated in the periphery than in the posterior pole. Histological studies have shown that the suprachoroid in the macula appears more as a transition zone between the loose collagen fibers of the choroid stroma and the more compact architecture of the sclera,[36] which is why pathologic suprachoroidal effusions tend to occur in the peripheral fundus. Hence, fluid injected into the suprachoroidal space may have a greater tendency to distribute circumferentially along the periphery rather than posteriorly toward

the macula.[35,38] In this way, suprachoroidal AAV delivery may be better suited for gene therapies that target peripheral or RPE diseases, or aimed at "biofactory" approaches such as the production of anti-angiogenesis agents for neovascular retinal conditions, rather than macular diseases or photoreceptor degenerations. Nevertheless, further optimization of suprachoroidal injection location, volume, or technique may improve delivery to the macular region. In this study, we chose AAV8 due to its similarity to AAV2, which has been widely used in clinical testing, and past studies demonstrating their greater efficacy in transducing photoreceptors and RPE as well as reduced immunogenicity when given subretinally in nonhuman primates.[46,51] Further testing of additional AAV serotypes, or methods to identify novel variants such as *in vivo*-directed evolution,[29] could help improve photoreceptor transduction from these transscleral approaches.

In our study, we found that *in vivo* transgene expression after suprachoroidal AAV8 delivery was transient, reaching maximal expression at 1 month but decreasing by months 2 and 3. The persistent expression in scleral cells at these latter time points suggests that the CMV promoter and transgene cassette remain active. Instead, the loss of expression over time may have resulted from cellular damage and phagocytic activity related to the local infiltration of inflammatory cells and disruption of RPE and photoreceptor segments, which appeared as early as 1 month after injection. Interestingly, while this localized chorioretinitis was not as apparent after subretinal or intravitreal delivery, we found that intravitreal AAV triggered more serum NAbs than did subretinal or suprachoroidal AAV. The distinct immune profiles with more localized inflammation after suprachoroidal AAV and greater systemic humoral immune response after intravitreal AAV help elucidate the immune consequences of AAV exposure to different compartments surrounding the outer BRB.

The BRB is composed of an inner barrier formed by endothelial tight junctions of retinal capillaries and an outer barrier of tight junctions in the RPE cell layer. Together, they provide a physical barrier that contributes in part to the immune-privileged status of the retina and subretinal space. Suprachoroidal injections expose AAV to resident macrophages in the choroid that likely function in immunosurveillance and pathogen detection of the extravascular milieu external to the outer BRB. This is evident from the preponderance of $Iba1^{+}$ cells, which, in the setting of significant RPE disruption, may include both choroidal macrophages and retinal microglia. At the same time, the extremely high blood flow through choroidal vessels—the highest of any tissue in the body[52]—likely limits the systemic exposure of viral vectors in the suprachoroidal space. In contrast, intravitreal AAVs exhibit greater biodistribution in systemic circulation akin to intravenous or intramuscular injections,[32] and they are associated with greater humoral and possibly cellular immune responses.[31,33,53] This is likely due to the greater trabecular outflow of AAV from the vitreous compared to the less efficient uveoscleral outflow through which suprachoroidal AAV could exit the eye. Hence, although AAV sequestration in the suprachoroidal space may lead to greater local inflammation, the higher systemic exposure of intravitreal AAV triggers a stronger systemic immune response, which may reduce the efficacy and durability of transgene expression.[54] Nevertheless, additional studies are necessary to address the local inflammation associated with suprachoroidal AAV delivery, as the distinct immune response compared with intravitreal AAV may warrant the use of local periocular or intraocular steroids rather than systemic immunosuppression. Newer AAV variants may also trigger a reduced immune response[51] and could result in less local inflammation if given suprachoroidally.

A previous study suggested the feasibility of delivering AAV5 to the suprachoroidal space using an illuminated microcatheter in rabbit eyes.[55] However, the blood supply to the rabbit retina is merangiotic, while humans and other primates have holangiotic retinal vasculature. A more recent study by Ding et al.[56] also demonstrated this approach in Norway brown rats, but the ocular dimensions of the rat eye are much smaller than humans and primates, and the suprachoroidal space is more difficult to access reliably. The team also employed a conventional 27-gauge needle to deliver AAV8 suprachoroidally in three nonhuman primates,[56] but this free-hand technique is less precise and cannot exclude the possibility of inadvertent subretinal delivery. In contrast, our study employed rhesus macaques with ocular dimensions and vasculature similar to humans, and transscleral microneedles, which reliably access the suprachoroidal space with well-characterized biodistribution,[57,58] and are already employed in human patients in phase I/II clinical trials.[42,59] We also employed *in vivo* SLO imaging, demonstrating the striking, unique expression pattern of suprachoroidal AAV8, consistent with the anatomic characteristics of the choroidal-scleral junction, which differs from subretinal or intravitreal AAV8 delivery.

In summary, we demonstrated a novel mode of AAV delivery using transscleral microneedles to access the subretinal or suprachoroidal space without the need for vitrectomy, retinotomy, or any surgical maneuvers. Suprachoroidal injections of AAV8 provide widespread, peripheral transgene expression in RPE, while subretinal AAV8 produces focal transduction of RPE and photoreceptors similar to conventional transretinal techniques. Although suprachoroidal AAV8 resulted in localized inflammation, the systemic humoral immune response was less pronounced than with intravitreal delivery. Our study intentionally avoided extensive immunosuppression in order to elucidate the native immune response to suprachoroidal AAV delivery. Thus, future studies evaluating additional AAV variants or employing local or systemic immunosuppression may unveil the true potential of this innovative approach.

MATERIALS AND METHODS

AAV8 Construct and Production

The AAV *cis* construct, which contained a CMV promoter, enhanced GFP transgene, woodchuck hepatitis virus post-transcriptional regulatory element (WPRE), and bovine growth hormone (bGH) polyadenylation signal, was packaged into AAV8 capsid and purified by the UC Davis NEI Vision Molecular Construct and Packaging Core according to the procedures described in Flannery and Visel.[60] Vector titer was

determined by TaqMan quantitative PCR, and purity was assessed by SDS-PAGE. The nonhuman primate-grade AAV8 was prepared using all endotoxin-free reagents. A single batch of AAV8 vectors was generated for this study, titered at 7.2×10^{13} vg/mL, stored in aliquots at −80°C, and thawed as needed for all experiments in this study to avoid freeze-thawing or potential variations in viral titer.

Ophthalmic Examinations and Study Schedule

Rhesus macaques selected for this study underwent ophthalmic examination at all time points. Ophthalmic imaging and aqueous fluid and serum collections were performed prior to AAV injections, and at 1 week, 1 month, and at the time of necropsy between 1 and 3 months. For examinations and procedures, animals were sedated with intramuscular injection of ketamine hydrochloride, midazolam, and dexmedetomidine, followed by pupillary dilation with phenylephrine (Paragon Biotech), tropicamide (Bausch & Lomb), and cyclopentolate (Akorn). Ophthalmic evaluations were conducted by portable slit lamp biomicroscopy (SL-7E, Topcon) of the anterior segment, and by indirect ophthalmoscopy (Heine) of the posterior pole. Anterior chamber inflammation was graded from portable slit lamp examination using SUN criteria for AC cells.[50] Vitreous inflammation was graded from indirect ophthalmoscopy using the National Eye Institute (NEI) scale reported by Nussenblatt et al.[61] for quantifying vitreous haze. IOP was measured by rebound tonometry (TonoVet, Icare). External photographs of the anterior segment were captured using a digital camera (Rebel T3, Canon). At study endpoint, a gross necropsy was performed to examine body surfaces, orifices, and cavities including heart, lungs, liver, stomach, kidney, spleen, pancreas, gonads, and brain. Eyes were collected in 4% paraformaldehyde immediately after euthanasia.

Intraocular Injections

After animal sedation, eyes were sterilely prepped with 1% povidone-iodine and flushed with sterile saline, followed by placement of an eyelid speculum. For transscleral microneedle injections, a 700 μm-long 30-gauge microneedle (Figure 1B, Clearside Biomedical) was inserted through the conjunctiva and sclera at 4 or 10 mm posterior to the corneal limbus to inject into the superotemporal quadrant (single 100-μL injection) of left eyes and into both the superotemporal and inferonasal quadrants (two 50-μL injections) of right eyes. For intravitreal injections, a 0.5-inch-long 30-gauge needle (BD Biosciences) was inserted through the pars plana, 4 mm posterior to the limbus, in the inferotemporal quadrant (single 100-μL injection) of both eyes. Anterior chamber taps were performed before and at all time points following AAV delivery to remove 150 μL of aqueous fluid using a 30-gauge needle for NAb testing. IOP was measured following intraocular injections, and additional aqueous was removed if necessary until the IOP was normalized. In rhesus 04, 05, and 06, a 40-mg periorbital subtenon injection of triamcinolone acetonide suspension (Kenalog-40, Bristol-Myers Squibb) was also performed in the superotemporal quadrant.

Ocular Imaging

All animals underwent SLO and SD-OCT using the Spectralis HRA+OCT device (Heidelberg Engineering) before and at 1 week, 1 month, and 2 or 3 months after AAV injections. Confocal SLO was used to capture 55° × 55° or 30° × 30° fluorescence images using 488-nm excitation light and a long-pass barrier filter starting at 500 nm. Images were captured from the central macula and from the peripheral retina by manually steering the Spectralis device. Due to the facial contour of these animals, the superior quadrants are more difficult to visualize. SD-OCT was performed alongside infrared reflectance images using an 820-nm diode laser to capture 30° × 5° SD-OCT raster scans with 1,536 A-scans per B-scan and 234 μm spacing between B-scans, in high-resolution mode. SD-OCT scans were captured from the central macula and in regions of visible GFP fluorescence, especially near the junction between transduced and untransduced tissues. 25 scans were averaged for each B-scan using the Heidelberg Engineering eye tracking automatic real-time (ART) software. Animals also underwent color fundus photography (CF-1, Canon) for documentation of clinical examination findings when possible.

Histology and Immunohistochemistry

Eyes were enucleated and placed in 4% paraformaldehyde (PFA) for less than 30 min, followed by gentle removal of anterior segments, including lens and vitreous. Whole eye cups were fixed in 4% PFA for 2 h at room temperature, rinsed with phosphate-buffered saline (PBS), cryoprotected with 30% sucrose overnight, embedded in optimal cutting temperature (OCT) medium, and then cryosectioned (18 μm) using a cryostat (CM3050 S, Leica). For immunohistochemistry, sections were washed with PBS, blocked with 10% normal donkey serum for 30 min, then incubated in primary antibody for 1–2 h at room temperature, followed by Alexa Fluor 568-conjugated secondary antibodies (Invitrogen). Primary antibodies include RPE65 (MAB5428, 1:250, Millipore), EGFP (Novousbio, NB100-1770, 1:500), IBA-1 (Wako, AB10558, 1:100), GFAP (Dako, Z0334, 1:200), CD45 (BD, 552566, 2.5 μg/mL), and CD3 (Abcam, ab11089, 1:100).

NAb Assays

NAb assays were performed on macaque sera or aqueous using an AAV transduction inhibition assay as previously described.[62] Briefly, 96-well plates were coated with poly-L-lysine (0.1 mg/mL), and HEK239T cells were seeded at 1×10^5 per well with DMEM containing 10% fetal bovine serum (FBS) at 37°C with 5% CO_2. The following day, cells were exposed to human adenovirus type 5 (VR-1516, ATCC) at an MOI of 90 for 2 h to increase susceptibility to AAV8. Aqueous or macaque sera were serially diluted from 1:5 to 1:2,560, mixed with AAV8-CMV-GFP virus at an MOI of 50,000, and then co-incubated at 37°C for 1 h. The serum-virus or aqueous-virus complexes were then incubated with the HEK293T cells for 48 h, and GFP^+ cells were detected with an inverted fluorescence microscope (Eclipse, Nikon). G-W ratios were calculated as the ratio of the aqueous NAb titer to the serum NAb titer.

Study Approval

The California National Primate Research Center (CNPRC) is accredited by the Association for Assessment and Accreditation of Laboratory Animal Care (AAALAC) International. All studies using rhesus macaques (*Macaca mulatta*) followed the guidelines of the

Association for Research in Vision and Ophthalmology (ARVO) Statement for the Use of Animals in Ophthalmic and Vision Research and complied with the National Institutes of Health (NIH) *Guide for the Care and Use of Laboratory Animals*. All procedures were conducted under protocols approved by the Institutional Animal Care and Use Committee (IACUC, protocol #20341).

SUPPLEMENTAL INFORMATION

Supplemental Information can be found online at https://doi.org/10.1016/j.omtm.2020.01.002.

AUTHOR CONTRIBUTIONS

G.Y. conceived the design, obtained funding, performed the examinations, intraocular injections, and *in vivo* imaging, and supervised the study. S.H.C. performed the histology, immunohistochemistry, and NAb assays. I.N.M. assisted with injections, *in vivo* imaging, and immunohistochemistry. U.T.N. assisted with histology and immunohistochemistry. S.M.T. assisted with examinations and injections. J.Y. assisted with injections. G.Y. drafted the manuscript, and G.Y., S.H.C., I.N.M., S.M.T., J.Y., D.T., and G.N. critically reviewed the manuscript.

CONFLICTS OF INTEREST

G.Y. received research support from Alcon, Clearside Biomedical, and Iridex, and personal fees for consultancy from Alimera, Allergan, Carl Zeiss Meditec, Genentech, and Iridex. D.T., J.Y., and G.N. are former employees at Clearside Biomedical, and have stock and issued and pending patents. Transscleral microneedles used in this study were provided by Clearside Biomedical, and may be requested under material transfer agreement (MTA). The remaining authors declare no competing interests.

ACKNOWLEDGMENTS

We thank Marie Burns and Huaiyang Chen for assistance with AAV8 production, Jeffrey Roberts and John Morrison for CNPRC logistics, Monica Motta for assistance with ocular imaging, Yevgeniy Sachnyev for help with image montage, Leah Byrne for discussions regarding AAV serotype choice, and Dennis J Hartigan-O'Connor for discussions on analyzing host immune responses. This study was supported by the California National Primate Research Center pilot grant program and base grant NIH P510D011107. G.Y. is supported by NIH K08 EY026101 and R21 EY031108, the E. Matilda Ziegler Foundation for the Blind, the Barr Foundation for Retinal Research, and by the Macula Society. S.T. is supported by NIH/NEI U24EY029904. AAV8 was produced by the Center for Vision Sciences Molecular Constructs and Packaging core facility supported by NIH P30 EY012576. No funding organizations had any role in the design or conduct of this research. The content is solely the responsibility of the authors and does not necessarily represent the official views of the funding agencies.

REFERENCES

1. Day, T.P., Byrne, L.C., Schaffer, D.V., and Flannery, J.G. (2014). Advances in AAV vector development for gene therapy in the retina. Adv. Exp. Med. Biol. *801*, 687–693.
2. Lebherz, C., Maguire, A., Tang, W., Bennett, J., and Wilson, J.M. (2008). Novel AAV serotypes for improved ocular gene transfer. J. Gene Med. *10*, 375–382.
3. Vandenberghe, L.H., and Auricchio, A. (2012). Novel adeno-associated viral vectors for retinal gene therapy. Gene Ther. *19*, 162–168.
4. Wu, Z., Asokan, A., and Samulski, R.J. (2006). Adeno-associated virus serotypes: vector toolkit for human gene therapy. Mol. Ther. *14*, 316–327.
5. Bainbridge, J.W., Mehat, M.S., Sundaram, V., Robbie, S.J., Barker, S.E., Ripamonti, C., Georgiadis, A., Mowat, F.M., Beattie, S.G., Gardner, P.J., et al. (2015). Long-term effect of gene therapy on Leber's congenital amaurosis. N. Engl. J. Med. *372*, 1887–1897.
6. Bainbridge, J.W., Smith, A.J., Barker, S.S., Robbie, S., Henderson, R., Balaggan, K., Viswanathan, A., Holder, G.E., Stockman, A., Tyler, N., et al. (2008). Effect of gene therapy on visual function in Leber's congenital amaurosis. N. Engl. J. Med. *358*, 2231–2239.
7. Maguire, A.M., Simonelli, F., Pierce, E.A., Pugh, E.N., Jr., Mingozzi, F., Bennicelli, J., Banfi, S., Marshall, K.A., Testa, F., Surace, E.M., et al. (2008). Safety and efficacy of gene transfer for Leber's congenital amaurosis. N. Engl. J. Med. *358*, 2240–2248.
8. Maguire, A.M., High, K.A., Auricchio, A., Wright, J.F., Pierce, E.A., Testa, F., Mingozzi, F., Bennicelli, J.L., Ying, G.S., Rossi, S., et al. (2009). Age-dependent effects of RPE65 gene therapy for Leber's congenital amaurosis: a phase 1 dose-escalation trial. Lancet *374*, 1597–1605.
9. Cideciyan, A.V., Hauswirth, W.W., Aleman, T.S., Kaushal, S., Schwartz, S.B., Boye, S.L., Windsor, E.A., Conlon, T.J., Sumaroka, A., Roman, A.J., et al. (2009). Vision 1 year after gene therapy for Leber's congenital amaurosis. N. Engl. J. Med. *361*, 725–727.
10. Hauswirth, W.W., Aleman, T.S., Kaushal, S., Cideciyan, A.V., Schwartz, S.B., Wang, L., Conlon, T.J., Boye, S.L., Flotte, T.R., Byrne, B.J., and Jacobson, S.G. (2008). Treatment of Leber congenital amaurosis due to *RPE65* mutations by ocular subretinal injection of adeno-associated virus gene vector: short-term results of a phase I trial. Hum. Gene Ther. *19*, 979–990.
11. Giacalone, J.C., Andorf, J.L., Zhang, Q., Burnight, E., Ochoa, D., Reutzel, A.J., Collins, M.M., Sheffield, V.C., Mullins, R.F., Han, I.C., et al. (2019). Development of a molecularly stable gene therapy vector for the treatment of RPGR-associated X-linked retinitis pigmentosa. Hum. Gene Ther. *30*, 967–974.
12. Cideciyan, A.V., Sudharsan, R., Dufour, V.L., Massengill, M.T., Iwabe, S., Swider, M., Lisi, B., Sumaroka, A., Marinho, L.F., Appelbaum, T., et al. (2018). Mutation-independent rhodopsin gene therapy by knockdown and replacement with a single AAV vector. Proc. Natl. Acad. Sci. USA *115*, E8547–E8556.
13. Beltran, W.A., Cideciyan, A.V., Boye, S.E., Ye, G.J., Iwabe, S., Dufour, V.L., Marinho, L.F., Swider, M., Kosyk, M.S., Sha, J., et al. (2017). Optimization of retinal gene therapy for X-linked retinitis pigmentosa due to *RPGR* mutations. Mol. Ther. *25*, 1866–1880.
14. Peters, T., Seitz, I.P., Michalakis, S., Biel, M., Wilhelm, B., Reichel, F., Ochakovski, G.A., Zrenner, E., Ueffing, M., Korbmacher, E., et al. (2019). Safety and toxicology of ocular gene therapy with recombinant AAV Vector rAAV.hCNGA3 in non-human primates. Hum. Gene Ther. Clin. Dev. Published online June 17, 2019. 10.1089.humc.2018.188.
15. Ye, G.J., Komáromy, A.M., Zeiss, C., Calcedo, R., Harman, C.D., Koehl, K.L., Stewart, G.A., Iwabe, S., Chiodo, V.A., Hauswirth, W.W., et al. (2017). Safety and efficacy of AAV5 vectors expressing human or canine CNGB3 in *CNGB3*-mutant dogs. Hum. Gene Ther. Clin. Dev. *28*, 197–207.
16. Cukras, C., Wiley, H.E., Jeffrey, B.G., Sen, H.N., Turriff, A., Zeng, Y., Vijayasarathy, C., Marangoni, D., Ziccardi, L., Kjellstrom, S., et al. (2018). Retinal AAV8-*RS1* gene therapy for X-linked retinoschisis: initial findings from a phase I/IIa trial by intravitreal delivery. Mol. Ther. *26*, 2282–2294.
17. Bush, R.A., Zeng, Y., Colosi, P., Kjellstrom, S., Hiriyanna, S., Vijayasarathy, C., Santos, M., Li, J., Wu, Z., and Sieving, P.A. (2016). Preclinical dose-escalation study of intravitreal AAV-RS1 gene therapy in a mouse model of X-linked retinoschisis: dose-dependent expression and improved retinal structure and function. Hum. Gene Ther. *27*, 376–389.
18. Grishanin, R., Vuillemenot, B., Sharma, P., Keravala, A., Greengard, J., Gelfman, C., Blumenkrantz, M., Lawrence, M., Hu, W., Kiss, S., and Gasmi, M. (2019). Preclinical evaluation of ADVM-022, a novel gene therapy approach to treating wet age-related macular degeneration. Mol. Ther. *27*, 118–129.

19. Rakoczy, E.P., Magno, A.L., Lai, C.M., Pierce, C.M., Degli-Esposti, M.A., Blumenkranz, M.S., and Constable, I.J. (2019). Three-year follow-up of phase 1 and 2a rAAV.sFLT-1 subretinal gene therapy trials for exudative age-related macular degeneration. Am. J. Ophthalmol. *204*, 113–123.

20. Constable, I.J., Pierce, C.M., Lai, C.M., Magno, A.L., Degli-Esposti, M.A., French, M.A., McAllister, I.L., Butler, S., Barone, S.B., Schwartz, S.D., et al. (2016). Phase 2a randomized clinical trial: safety and post hoc analysis of subretinal rAAV.sFLT-1 for wet age-related macular degeneration. EBioMedicine *14*, 168–175.

21. Medawar, P.B. (1948). Immunity to homologous grafted skin; the fate of skin homografts transplanted to the brain, to subcutaneous tissue, and to the anterior chamber of the eye. Br. J. Exp. Pathol. *29*, 58–69.

22. Streilein, J.W. (2003). Ocular immune privilege: therapeutic opportunities from an experiment of nature. Nat. Rev. Immunol. *3*, 879–889.

23. Fisher, S.K., Lewis, G.P., Linberg, K.A., Barawid, E., and Verardo, M.R. (2007). Cellular remodeling in mammalian retina induced by retinal detachment. In Webvision: The Organization of the Retina and Visual System [Internet], H. Kolb, E. Fernandez, and R. Nelson, eds. (University of Utah Health Sciences Center), https://www.ncbi.nlm.nih.gov/books/NBK11552/.

24. Russell, S., Bennett, J., Wellman, J.A., Chung, D.C., Yu, Z.F., Tillman, A., Wittes, J., Pappas, J., Elci, O., McCague, S., et al. (2017). Efficacy and safety of voretigene neparvovec (AAV2-hRPE65v2) in patients with *RPE65*-mediated inherited retinal dystrophy: a randomised, controlled, open-label, phase 3 trial. Lancet *390*, 849–860.

25. Todorich, B., Yiu, G., and Hahn, P. (2014). Current and investigational pharmacotherapeutic approaches for modulating retinal angiogenesis. Expert Rev. Clin. Pharmacol. *7*, 375–391.

26. Dalkara, D., Kolstad, K.D., Caporale, N., Visel, M., Klimczak, R.R., Schaffer, D.V., and Flannery, J.G. (2009). Inner limiting membrane barriers to AAV-mediated retinal transduction from the vitreous. Mol. Ther. *17*, 2096–2102.

27. Teo, K.Y.C., Lee, S.Y., Barathi, A.V., Tun, S.B.B., Tan, L., and Constable, I.J. (2018). Surgical removal of internal limiting membrane and layering of AAV vector on the retina under air enhances gene transfection in a nonhuman primate. Invest. Ophthalmol. Vis. Sci. *59*, 3574–3583.

28. Takahashi, K., Igarashi, T., Miyake, K., Kobayashi, M., Yaguchi, C., Iijima, O., Yamazaki, Y., Katakai, Y., Miyake, N., Kameya, S., et al. (2017). Improved intravitreal AAV-mediated inner retinal gene transduction after surgical internal limiting membrane peeling in cynomolgus monkeys. Mol. Ther. *25*, 296–302.

29. Dalkara, D., Byrne, L.C., Klimczak, R.R., Visel, M., Yin, L., Merigan, W.H., Flannery, J.G., and Schaffer, D.V. (2013). In vivo-directed evolution of a new adeno-associated virus for therapeutic outer retinal gene delivery from the vitreous. Sci. Transl. Med. *5*, 189ra76.

30. Petrs-Silva, H., Dinculescu, A., Li, Q., Deng, W.T., Pang, J.J., Min, S.H., Chiodo, V., Neeley, A.W., Govindasamy, L., Bennett, A., et al. (2011). Novel properties of tyrosine-mutant AAV2 vectors in the mouse retina. Mol. Ther. *19*, 293–301.

31. Li, Q., Miller, R., Han, P.Y., Pang, J., Dinculescu, A., Chiodo, V., and Hauswirth, W.W. (2008). Intraocular route of AAV2 vector administration defines humoral immune response and therapeutic potential. Mol. Vis. *14*, 1760–1769.

32. Seitz, I.P., Michalakis, S., Wilhelm, B., Reichel, F.F., Ochakovski, G.A., Zrenner, E., Ueffing, M., Biel, M., Wissinger, B., Bartz-Schmidt, K.U., et al.; RD-CURE Consortium (2017). Superior retinal gene transfer and biodistribution profile of subretinal versus intravitreal delivery of AAV8 in nonhuman primates. Invest. Ophthalmol. Vis. Sci. *58*, 5792–5801.

33. Reichel, F.F., Peters, T., Wilhelm, B., Biel, M., Ueffing, M., Wissinger, B., Bartz-Schmidt, K.U., Klein, R., Michalakis, S., and Fischer, M.D.; RD-CURE Consortium (2018). Humoral immune response after intravitreal but not after subretinal AAV8 in primates and patients. Invest. Ophthalmol. Vis. Sci. *59*, 1910–1915.

34. Reichel, F.F., Dauletbekov, D.L., Klein, R., Peters, T., Ochakovski, G.A., Seitz, I.P., Wilhelm, B., Ueffing, M., Biel, M., Wissinger, B., et al.; RD-CURE Consortium (2017). AAV8 can induce innate and adaptive immune response in the primate eye. Mol. Ther. *25*, 2648–2660.

35. Moisseiev, E., Loewenstein, A., and Yiu, G. (2016). The suprachoroidal space: from potential space to a space with potential. Clin. Ophthalmol. *10*, 173–178.

36. Yiu, G., Pecen, P., Sarin, N., Chiu, S.J., Farsiu, S., Mruthyunjaya, P., and Toth, C.A. (2014). Characterization of the choroid-scleral junction and suprachoroidal layer in healthy individuals on enhanced-depth imaging optical coherence tomography. JAMA Ophthalmol. *132*, 174–181.

37. Willoughby, A.S., Vuong, V.S., Cunefare, D., Farsiu, S., Noronha, G., Danis, R.P., and Yiu, G. (2018). Choroidal changes after suprachoroidal injection of triamcinolone acetonide in eyes with macular edema secondary to retinal vein occlusion. Am. J. Ophthalmol. *186*, 144–151.

38. Emami-Naeini, P., and Yiu, G. (2019). Medical and surgical applications for the suprachoroidal space. Int. Ophthalmol. Clin. *59*, 195–207.

39. Olsen, T.W., Feng, X., Wabner, K., Conston, S.R., Sierra, D.H., Folden, D.V., Smith, M.E., and Cameron, J.D. (2006). Cannulation of the suprachoroidal space: a novel drug delivery methodology to the posterior segment. Am. J. Ophthalmol. *142*, 777–787.

40. Patel, S.R., Lin, A.S., Edelhauser, H.F., and Prausnitz, M.R. (2011). Suprachoroidal drug delivery to the back of the eye using hollow microneedles. Pharm. Res. *28*, 166–176.

41. Kim, Y.C., Edelhauser, H.F., and Prausnitz, M.R. (2014). Targeted delivery of antiglaucoma drugs to the supraciliary space using microneedles. Invest. Ophthalmol. Vis. Sci. *55*, 7387–7397.

42. Campochiaro, P.A., Wykoff, C.C., Brown, D.M., Boyer, D.S., Barakat, M., Taraborelli, D., and Noronha, G.; Tanzanite Study Group (2018). Suprachoroidal triamcinolone acetonide for retinal vein occlusion: results of the Tanzanite Study. Ophthalmol. Retina *2*, 320–328.

43. Yeh, S., Kurup, S.K., Wang, R.C., Foster, C.S., Noronha, G., Nguyen, Q.D., and Do, D.V.; DOGWOOD Study Team (2019). Suprachoroidal injection of triamcinolone acetonide, CLS-TA, for macular edema due to noninfectious uveitis: a randomized, phase 2 study (DOGWOOD). Retina *39*, 1880–1888.

44. Yiu, G., Vuong, V.S., Oltjen, S., Cunefare, D., Farsiu, S., Garzel, L., Roberts, J., and Thomasy, S.M. (2016). Effect of uveal melanocytes on choroidal morphology in rhesus macaques and humans on enhanced-depth imaging optical coherence tomography. Invest. Ophthalmol. Vis. Sci. *57*, 5764–5771.

45. Yiu, G., Wang, Z., Munevar, C., Tieu, E., Shibata, B., Wong, B., Cunefare, D., Farsiu, S., Roberts, J., and Thomasy, S.M. (2018). Comparison of chorioretinal layers in rhesus macaques using spectral-domain optical coherence tomography and high-resolution histological sections. Exp. Eye Res. *168*, 69–76.

46. Vandenberghe, L.H., Bell, P., Maguire, A.M., Cearley, C.N., Xiao, R., Calcedo, R., Wang, L., Castle, M.J., Maguire, A.C., Grant, R., et al. (2011). Dosage thresholds for AAV2 and AAV8 photoreceptor gene therapy in monkey. Sci. Transl. Med. *3*, 88ra54.

47. Calcedo, R., Chichester, J.A., and Wilson, J.M. (2018). Assessment of humoral, innate, and T-cell immune responses to adeno-associated virus vectors. Hum. Gene Ther. Methods *29*, 86–95.

48. Perocheau, D.P., Cunningham, S., Lee, J., Antinao Diaz, J., Waddington, S.N., Gilmour, K., Eaglestone, S., Lisowski, L., Thrasher, A.J., Alexander, I.E., et al. (2019). Age-related seroprevalence of antibodies against AAV-LK03 in a UK population cohort. Hum. Gene Ther. *30*, 79–87.

49. Yiu, G., Tieu, E., Munevar, C., Wong, B., Cunefare, D., Farsiu, S., Garzel, L., Roberts, J., and Thomasy, S.M. (2017). In vivo multimodal imaging of drusenoid lesions in rhesus macaques. Sci. Rep. *7*, 15013.

50. Jabs, D.A., Nussenblatt, R.B., and Rosenbaum, J.T.; Standardization of Uveitis Nomenclature (SUN) Working Group (2005). Standardization of uveitis nomenclature for reporting clinical data. Results of the First International Workshop. Am. J. Ophthalmol. *140*, 509–516.

51. Ramachandran, P.S., Lee, V., Wei, Z., Song, J.Y., Casal, G., Cronin, T., Willett, K., Huckfeldt, R., Morgan, J.I., Aleman, T.S., et al. (2017). Evaluation of dose and safety of AAV7m8 and AAV8BP2 in the non-human primate retina. Hum. Gene Ther. *28*, 154–167.

52. Nickla, D.L., and Wallman, J. (2010). The multifunctional choroid. Prog. Retin. Eye Res. *29*, 144–168.

53. Maclachlan, T.K., Lukason, M., Collins, M., Munger, R., Isenberger, E., Rogers, C., Malatos, S., Dufresne, E., Morris, J., Calcedo, R., et al. (2011). Preclinical safety evaluation of AAV2-sFLT01—a gene therapy for age-related macular degeneration. Mol. Ther. *19*, 326–334.

54. Kotterman, M.A., Yin, L., Strazzeri, J.M., Flannery, J.G., Merigan, W.H., and Schaffer, D.V. (2015). Antibody neutralization poses a barrier to intravitreal adeno-associated viral vector gene delivery to non-human primates. Gene Ther. *22*, 116–126.

55. Peden, M.C., Min, J., Meyers, C., Lukowski, Z., Li, Q., Boye, S.L., Levine, M., Hauswirth, W.W., Ratnakaram, R., Dawson, W., et al. (2011). Ab-externo AAV-mediated gene delivery to the suprachoroidal space using a 250 micron flexible microcatheter. PLoS ONE *6*, e17140.

56. Ding, K., Shen, J., Hafiz, Z., Hackett, S.F., Silva, R.L.E., Khan, M., Lorenc, V.E., Chen, D., Chadha, R., Zhang, M., et al. (2019). AAV8-vectored suprachoroidal gene transfer produces widespread ocular transgene expression. J. Clin. Invest. *130*, 4901–4911.

57. Chiang, B., Venugopal, N., Edelhauser, H.F., and Prausnitz, M.R. (2016). Distribution of particles, small molecules and polymeric formulation excipients in the suprachoroidal space after microneedle injection. Exp. Eye Res. *153*, 101–109.

58. Chiang, B., Wang, K., Ethier, C.R., and Prausnitz, M.R. (2017). Clearance kinetics and clearance routes of molecules from the suprachoroidal space after microneedle injection. Invest. Ophthalmol. Vis. Sci. *58*, 545–554.

59. Wykoff, C.C., Khurana, R.N., Lampen, S.I.R., Noronha, G., Brown, D.M., Ou, W.C., and Sadda, S.R.; HULK Study Group (2018). Suprachoroidal triamcinolone acetonide for diabetic macular edema: the HULK Trial. Ophthalmol. Retina *2*, 874–877.

60. Flannery, J.G., and Visel, M. (2013). Adeno-associated viral vectors for gene therapy of inherited retinal degenerations. Methods Mol. Biol. *935*, 351–369.

61. Nussenblatt, R.B., Palestine, A.G., Chan, C.C., and Roberge, F. (1985). Standardization of vitreal inflammatory activity in intermediate and posterior uveitis. Ophthalmology *92*, 467–471.

62. Day, T.P., Byrne, L.C., Flannery, J.G., and Schaffer, D.V. (2018). Screening for neutralizing antibodies against natural and engineered AAV capsids in nonhuman primate retinas. Methods Mol. Biol. *1715*, 239–249.

OMTM, Volume *16*

Supplemental Information

Suprachoroidal and Subretinal Injections of AAV Using Transscleral Microneedles for Retinal Gene Delivery in Nonhuman Primates

Glenn Yiu, Sook Hyun Chung, Iris N. Mollhoff, Uyen Tu Nguyen, Sara M. Thomasy, Jesse Yoo, Donna Taraborelli, and Glenn Noronha

Supplementary Materials

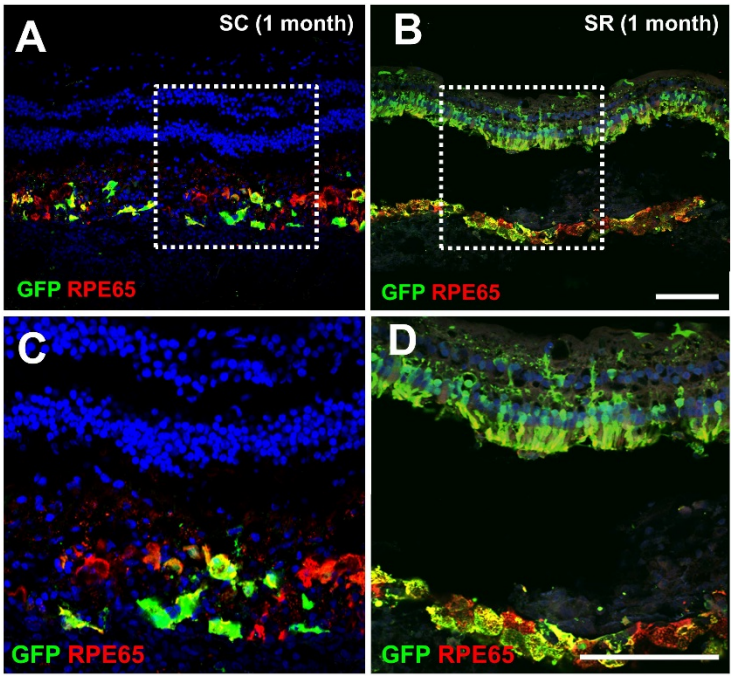

Fig S1. Retinal anatomy and GFP expression near injection sites after suprachoroidal and subretinal injection of AAV8 in rhesus macaques. **(A-B)** Confocal fluorescence images with **(C-D)** magnified views of the white-dashed boxes in (A-B) showing GFP expression (green) co-immunostained with anti-RPE65 (red) to label retinal pigment epithelium (RPE) in areas of retinal structure disruption near injection sites after suprachoroidal (A, C) or subretinal (B, D) injections of AAV8. Scale bars: 100 μm.

A

ID	Eye	Dose (vg/eye)	Injectant Location	Pre-injection AC Cell	1 Week AC Cell	2 Week AC Cell	1 Month AC Cell	2 Months AC Cell	3 Months AC Cell
Rhesus 01	OD	7×10^{11}	SC	0	0.5	0	0		0
	OS	7×10^{11}	SC	0	0	0	0		0
Rhesus 02	OD	7×10^{12}	SC	0	0.5	2*	0		0
	OS	7×10^{12}	SC	0	0.5	2*	0		0
Rhesus 03	OD	7×10^{12}	SR	0#	0	0	0	0	
	OS	7×10^{12}	SC	0#	0	0	0	0	
Rhesus 04	OD	7×10^{12}	SR	0#	0	0	0		
	OS	7×10^{12}	SC	0#	0	0	0		
Rhesus 05	OD	7×10^{12}	IVT	0#	0	0	0		
	OS	7×10^{12}	IVT	0#	0	0	0		

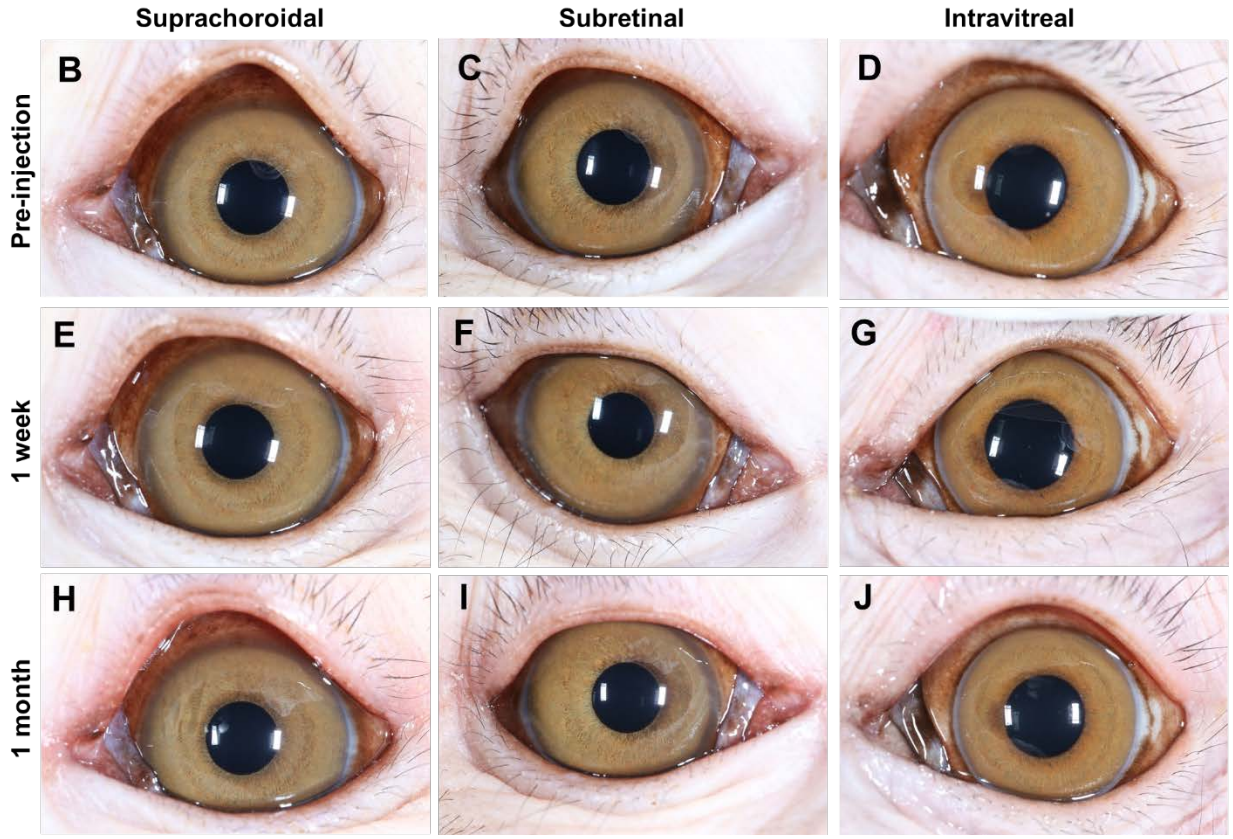

Fig S2. Anterior chamber inflammation following suprachoroidal, subretinal, and intravitreal injections of AAV8. **(A)** Table outlining study animals and eyes, AAV8 dose, injectant location, and degree of anterior chamber (AC) cell before and after intraocular injections. AC cells were graded based on Standardization of Uveitis Nomenclature (SUN) criteria. *Rhesus 02 exhibited AC inflammation at 2 weeks and was treated oral prednisone (1mg/kg), while #subsequent animals received periorbital subtenon triamcinolone acetate (40mg) at time of the AAV8 injection. **(B-J)** Representative external photographs show minimal anterior uveitis before (B-D), and at 1 week (E-G) or 1 month (H-J) after suprachoroidal (B, E, H), subretinal (C, F, I) or intravitreal (D, G, J) injections of AAV8.

A

ID	Eye	Dose (vg/eye)	Injectant Location	Pre-injection Vitreous Haze	1 Week Vitreous Haze	2 Week Vitreous Haze	1 Month Vitreous Haze	2 Months Vitreous Haze	3 Months Vitreous Haze
Rhesus 01	OD	7×10^{11}	SC	0	0	0	0		0
	OS	7×10^{11}	SC	0	0	0	0		0
Rhesus 02	OD	7×10^{12}	SC	0	0	0	0		0
	OS	7×10^{12}	SC	0	0	0	0		0
Rhesus 03	OD	7×10^{12}	SR	0	0	0	0	0	
	OS	7×10^{12}	SC	0	0	0	0	0	
Rhesus 04	OD	7×10^{12}	SR	0	0	0	0		
	OS	7×10^{12}	SC	0	0	0	0		
Rhesus 05	OD	7×10^{12}	IVT	0	0	0	0		
	OS	7×10^{12}	IVT	0	0	0	0		

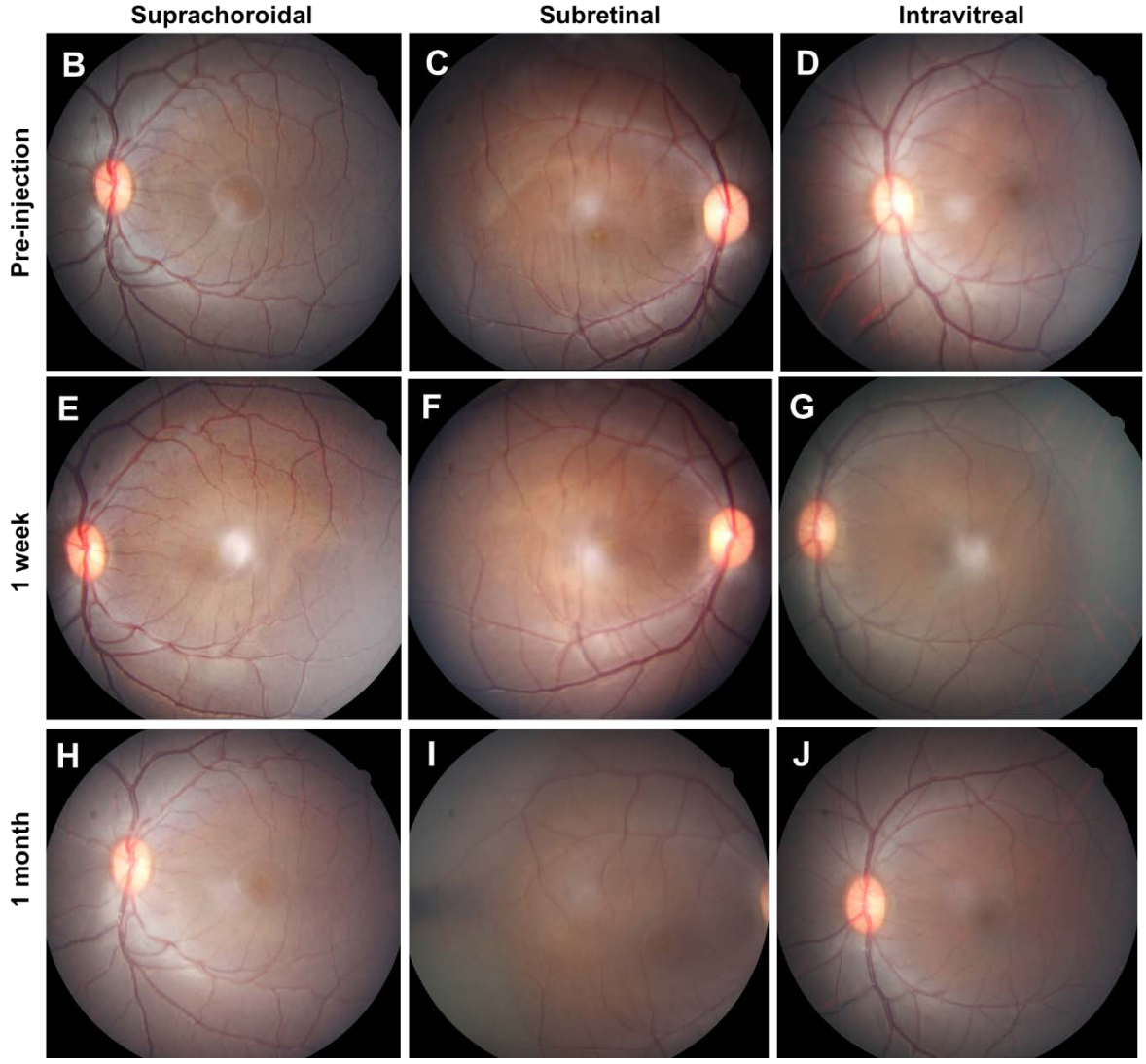

Fig S3. Posterior inflammation following suprachoroidal, subretinal, and intravitreal injections of AAV8. **(A)** Table outlining study animals and eyes, AAV8 dose, injectant location, and vitreous haze before and after intraocular injections. Vitreous inflammation was graded based on National Eye Institute (NEI) scale for vitreous haze. **(B-J)** Representative fundus photographs show minimal vitritis before (B-D), and at 1 week (E-G) or 1 month (H-J) after suprachoroidal (B, E, H), subretinal (C, F, I) or intravitreal (D, G, J) injections of AAV8.

Table S1. Intraocular pressure after suprachoroidal, subretinal, or intravitreal AAV8 injections

ID	Eye	Dose (vg/eye)	Injectant Location	Pre-injection IOP	1 Week IOP	1 Month IOP	2 Months IOP	3 Months IOP
Rhesus 01	OD	7×10^{11}	SC	14	7	7		14
	OS	7×10^{11}	SC	19	10	8		20
Rhesus 02	OD	7×10^{12}	SC	17	13	23		13
	OS	7×10^{12}	SC	18	18	23		15
Rhesus 03	OD	7×10^{12}	SR	19	16	16	21	
	OS	7×10^{12}	SC	24	19	19	19	
Rhesus 04	OD	7×10^{12}	SR	14	13	18		
	OS	7×10^{12}	SC	17	15	16		
Rhesus 05	OD	7×10^{12}	IVT	21	15	15		
	OS	7×10^{12}	IVT	19	14	14		